Original Article

Predicting malignancy: subsolid nodules detected on LDCT in a surgical cohort of East Asian patients

Yung-Hsien Wang[1], Chieh-Feng Chen[2,3,4,5,6], Yen-Kuang Lin[7,8], Caleb Chiang[9], Ching Tzao[10#], Yun Yen[1,11,12,13#]

[1]TMU Research Center of Cancer Translational Medicine, [2]Graduate Institute of Clinical Medicine, College of Medicine, [3]Department of Public Health, College of Medicine, [4]Cochrane Taiwan, Taipei Medical University, Taipei; [5]Division of Plastic Surgery, [6]Evidence-Based Medicine Center, Wan Fang Hospital, Taipei Medical University, Taipei; [7]Biostatistics Research Center, [8]School of Nursing, College of Nursing, Taipei Medical University, Taipei; [9]Trinity College of Arts & Sciences, Duke University, Durham, USA; [10]Division of Thoracic Surgery, Kuang Tien General Hospital, Taichung; [11]PhD Program for Cancer Biology and Drug Discovery, College of Medical Science and Technology, [12]Graduate Institute of Cancer Biology and Drug Discovery, Taipei Medical University, Taipei; [13]Cancer Center, Taipei Municipal Wan Fang Hospital, Taipei

Contributions: (I) Conception and design: All authors; (II) Administrative support: CF Chen, C Tzao, Y Yen; (III) Provision of study materials or patients: C Tzao; (IV) Collection and assembly of data: YH Wang, C Tzao; (V) Data analysis and interpretation: YH Wang, YK Lin; (VI) Manuscript writing: All authors; (VII) Final approval of manuscript: All authors.

[#]These authors contributed equally to this work.

Correspondence to: Yun Yen, MD, PhD. Department of Cancer Biology and Drug Discovery, College of Medical Technology, Taipei Medical University, 250 Wuxing St, Xinyi District, Taipei. Email: y.yenmd@gmail.com; Ching Tzao, MD, PhD. Division of Thoracic Surgery, Kuang Tien General Hospital, No.117, Shatian Road, Shalu District, Taichung City. Email: tzao@yahoo.com.

Background: Due to widespread use of low-dose computed tomography (LDCT) screening, increasing number of patients are found to have subsolid nodules (SSNs). The management of SSNs is a clinical challenge and primarily depends on CT imaging. We seek to identify risk factors that may help clinicians determine an optimal course of management.

Methods: We retrospectively reviewed the characteristics of 83 SSN lesions, including 48 pure ground-glass nodules and 35 part-solid nodules, collected from 83 patients who underwent surgical resection.

Results: Of the 83 SSNs, 16 (19.28%) were benign and 67 (80.72%) were malignant, including 23 adenocarcinomas in situ (AIS), 16 minimally invasive adenocarcinomas (MIA), and 28 invasive adenocarcinomas (IA). Malignant lesions were found to have significantly larger diameters (P<0.05) with an optimal cut-off point of 9.24 mm. Significant indicators of malignancy include female sex (P<0.05), air bronchograms (P<0.001), spiculation (P<0.05), pleural tail sign (P<0.05), and lobulation (P<0.05). When compared with AIS/MIA combined, IA lesions were found to be larger (P<0.05) with an optimal cut-off of 12 mm, and have a higher percentage of part-solid nodules (P<0.001), pleural tail sign (P<0.001), air bronchograms (P<0.05), and lobulation (P<0.05). Further multivariate analysis found that lesion size and spiculation were independent factors for malignancy while part-solid nodules were associated with IA histology.

Conclusions: East Asian females are at risk of presenting with a malignant lesion even without history of heavy smoking or old age. Nodule features associated with malignancy include larger size, air bronchograms, lobulation, pleural tail sign, spiculation, and solid components. A combination of patient characteristic and LDCT features can be effectively used to guide management of patients with SSNs.

Keywords: Ground-glass opacity (GGO); subsolid nodules (SSNs); lung adenocarcinoma; computed tomography

Submitted Jan 22, 2020. Accepted for publication Jun 19, 2020.
doi: 10.21037/jtd-20-659
View this article at: http://dx.doi.org/10.21037/jtd-20-659

Introduction

With the growing use of low-dose computed tomography (LDCT) lung cancer screening, small subsolid nodules (SSNs) have been frequently found as precursors to early-stage malignancy. SSNs are defined as focal areas of increased attenuation or haziness through which normal airway and vascular parenchyma can be visualized (1). They can be further categorized as pure ground-glass nodules (pGGNs) or part-solid nodules (PSNs) depending on the presence of additional solid components observed on the mediastinal window.

SSNs merit special consideration as they are detected in CT studies with a prevalence of 2–4% in screened populations (2,3) and may represent either benign or malignant changes. Their etiologies often include nonmalignant focal fibrosis, premalignant atypical adenomatous hyperplasia (AAH), adenocarcinoma *in situ* (AIS), minimally invasive adenocarcinoma (MIA), and invasive adenocarcinoma (IA) (1) (*Figure 1*). According to the 2011 International Association for the Study of Lung Cancer (IASLC) lung adenocarcinoma classification (4), AAH is a small (usually ≤5 mm) proliferation of mildly atypical type II pneumocytes or Clara cells that line alveolar walls, and is analogous to squamous dysplasia. AIS, one of the lesions formerly classified as bronchioloalveolar carcinoma (BAC), is a localized adenocarcinoma ≤3 cm showing neoplastic growth along preexisting alveolar structures (i.e., lepidic growth), without any stromal, vascular, or pleural invasion. MIA, in contrast, is an adenocarcinoma, with a predominantly lepidic pattern and invasion ≤5 mm in greatest dimension in any one focus. Tumors with more than 5 mm of invasion are classified as IA and can be subsequently categorized with comprehensive histological subtyping into lepidic predominant, acinar predominant, papillary predominant, micropapillary predominant, and solid predominant with mucin production.

The management of SSN cases proves to be challenging. Approximately 75% of SSNs found at baseline can persist for over 3 months (3) and 26–28% can show significant growth of more than 2 mm within 2–4 years (5,6). The indication for invasive intervention is mainly based on CT features (7), which are observer-dependent and exhibit varied predictive values. Furthermore, lung cancers in the form of SSNs generally follow an indolent course and grow slowly. With a mean volume doubling time (VDT) of up to 1,041 days and with 2–3% of persistent nodules showing significant growth after 3–4 years of stability (5,8), it is difficult to determine optimal timings for follow-up examinations.

Since current management guidelines for SSNs are largely based on studies on Japanese and Korean

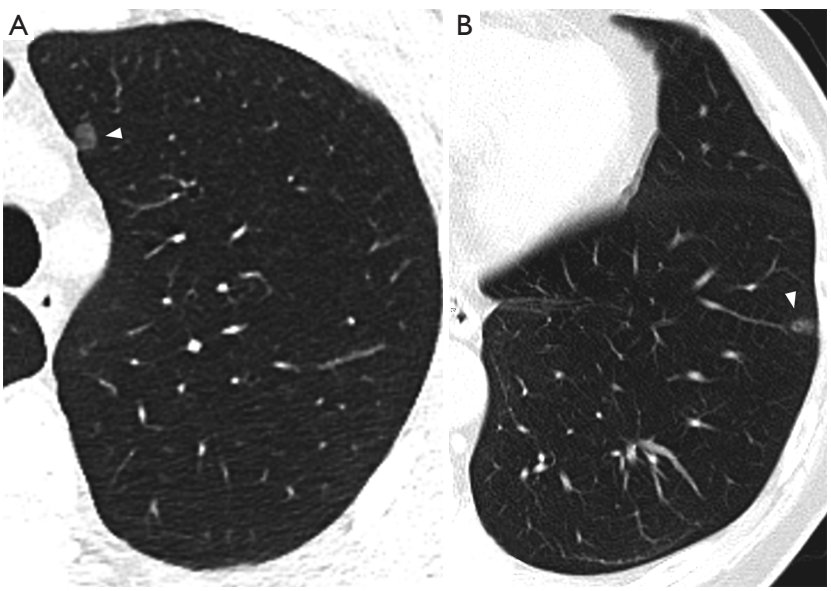

Figure 1 Benign and malignant lesions presenting as pGGNs. (A) AAH presenting as a 6.4 mm well-defined pGGN (white arrowhead) in the LUL of a 44-year-old male. (B) Invasive adenocarcinoma presenting as an 8 mm well-defined pGGN (white arrowhead) with air bronchograms in the LLL of a 68-year-old male. AAH, atypical adenomatous hyperplasia; LUL, left upper lobe; LLL, left lower lobe.

populations, it is also necessary to consider the potential difference in epidemiology and clinical presentations among different populations. For example, prior studies have elucidated differences in adenocarcinoma characteristics between Asians and Caucasians. Specifically, lung cancer in never-smokers (LCNS), characteristic of Asian females, is a clinically distinct entity that predominantly comprises adenocarcinomas with a high prevalence of EGFR mutation and a younger patient population (9). In this study, our goal is to explore the clinical and imaging characteristics of SSNs in the Taiwanese population while validating the distinct factors that help differentiate between benign and malignant lesions. We present the following article in accordance with the STROBE reporting (available at http://dx.doi.org/10.21037/jtd-20-659).

Methods

Patients

We retrospectively reviewed thoracic surgical data between June 2015 and June 2019 and identified a consecutive series of 83 patients who underwent surgical removal and pathological diagnosis of SSNs detected by LDCT during self-enrolled medical check-ups. The indication for invasive interventions was determined by a combination of imaging features and patient characteristics such as lesion size, lesion morphology, and patient history. All patients who chose invasive intervention underwent surgical resection. This study was conducted in accordance with the Declaration of Helsinki (as revised in 2013) and approved by the Joint Institutional Review Board at Taipei Medical University (TMU-JIRB; No. N201909060). The requirement of informed consent was waived.

CT examination

CT scans were obtained using a second-generation, dual-source CT system (SOMATOM Definition Flash, Siemens Healthcare, Forchheim, Germany) with the following parameters: 0.6 mm section thickness, 120 kV tube voltage, 20 mA tube current, and 0.33 seconds scanning time. Images were displayed using lung window [width: 1,200 Hounsfield units (HU); level: –600 HU] and mediastinal window settings (width: 350 HU; level: 50 HU). All images and findings were interpreted and recorded by a thoracic surgery specialist with 30 years of experience immediately before lesions underwent pathological diagnosis. Pure GGNs were defined as focal areas of increased attenuation without any solid components on the lung window through which normal vascular and bronchial parenchyma are visible. Nodules were classified as PSNs if solid components visible on the mediastinal window were present in ground-glass lesions. We evaluated the maximum nodule diameter, air bronchograms, spiculation, lobulation, ill-defined margins, and pleural tail sign (*Figure 2*). Air bronchograms, including dot-like bubble lucencies, were defined as areas of air attenuation within the opacified SSN. Spiculation was defined as spike-like protrusions extending from the lesion margin. Lobulation was defined as lesion margins with bulging or scalloped edges. Margins were described as ill-defined if lesion contours were not clearly demarcated or easily distinguishable. Lastly, pleural tail signs were defined as linear opacities arising from nodules that extend towards nearby pleura, sometimes causing pleural retraction or indentation.

Surgery and pathology

All pathological specimens were acquired by video-assisted thoracoscopic surgery. Seven patients underwent lobectomy and 76 underwent sublobar resection (13 segmentectomies and 63 wedge resections). Thirteen patients had a second or third lesion located in the same lobe that was simultaneously resected. Among these patients, only the larger lesion of each individual was included in the study. Pathological diagnosis was performed by four pathologists with 25 to 35 years of experience and followed the 2011 IASLC adenocarcinoma classification (4).

Statistical analysis

Statistical analysis was performed using SAS v.9.4 (version 9.4, SAS Institute Inc., Cary, USA). The mean, median, and standard deviation for patient age and largest nodule diameter were calculated, and comparisons of continuous data between malignant and benign lesions were conducted using Student's *t*-test. Categorical data were analyzed with Pearson's χ^2 test. Optimal cut-offs were determined using receiver operating characteristic (ROC) curve analysis and the Youden's J index. A P value less than 0.05 was considered statistically significant. For significant variables, the odds ratios (OR) were calculated using univariate logistic regression, and multivariate logistic regression was performed for malignancy and IA histology. Additional sensitivity analyses on subjects who were younger than

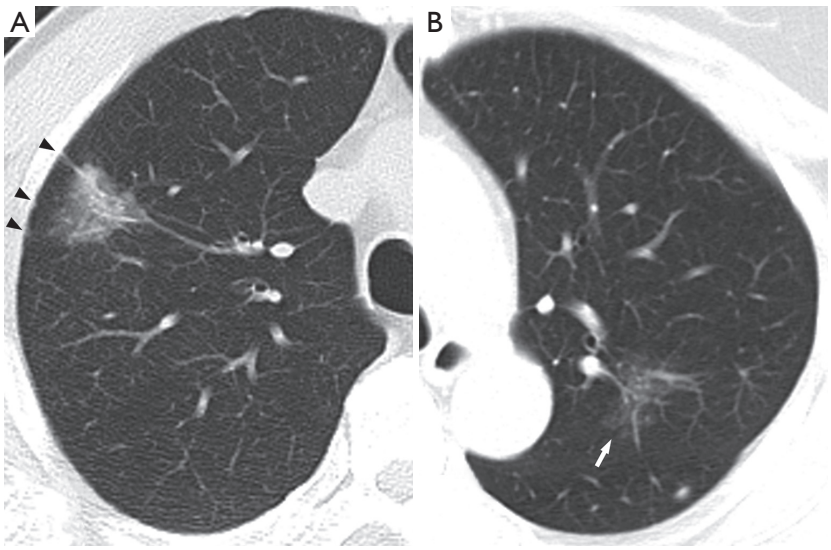

Figure 2 Imaging characteristics of subsolid nodules. (A) Invasive adenocarcinoma presenting as a 20 mm PSN with ill-defined margins, air bronchograms, spiculation, and pleural tail signs accompanied with pleural retraction (black arrowheads) in the RUL of a 59-year-old male. (B) AIS presenting as a 22 mm pGGN with ill-defined margins and lobulation (white arrow) in the LUL of a 69-year-old female. PSN, part-solid nodule; RUL, right upper lobe; AIS, adenocarcinoma in situ; pGGN, pure ground-glass nodule; LUL, left upper lobe.

Table 1 Characteristics of the 83 study patients

Characteristics	n	%
Age (year)*	55.76±10.82	28–79
Female sex	50	60.24
Smoking history		
Never-smoker	69	83.13
Ex-smoke	12	14.46
Current smoker	2	2.41
Multiple nodules	13	15.66
History of malignancy	15	18.07

n, number of cases. *, data presented as mean ± standard deviation, range.

65 years old or never-smokers showed results consistent with the whole sample.

Results

Patients

Characteristics of the patient sample are summarized in *Table 1*. The patient sample consists of 50 females (60.24%) and 33 males, with a mean age of 55.76 years (standard deviation 10.82, median 57 years, range 28–79 years). Thirteen males and 1 female were ever-smokers with a mean pack years (PY) of 27.5±10.1 PY (median 25 PY, range 15–50 PY). All ever-smokers have quit for more than 15 years. Thirteen patients had multiple SSNs, and only the largest lesions in each of these patients were evaluated. Fifteen patients had a history of treated malignancy, including five breast cancer cases, four colon cancers, three lung adenocarcinomas, one gastric adenocarcinoma, one endometrial cancer, and one adrenal cancer.

Nodule characteristics

Table 2 shows the nodule characteristics of the 83 nodules that were analyzed, including 47 LUNG-RADS 2 (all pGGNs); 22 Lung-RADS 3 (1 pGGN, 21 PSN); 6 Lung-RADS 4a (all PSNs); 8 Lung-RADS 4b (all PSNs). The mean nodule size was 12.01±7.23 mm (median 9.74 mm, range 5–48 mm) for the largest diameters. Forty-right nodules were pGGNs (57.83%) and 35 were PSNs (42.17%). Forty-seven nodules were found to be located in the upper lobes (56.63%) and 44 were found in the right lobes (53.01%). Pathologic diagnosis showed that 16 lesions were benign and consisted of fibrosis in four patients, AAH in six patients, intrapulmonary lymph node in two patients, interstitial pneumonitis in one patient, Cryptococcus

Table 2 Characteristics of the 83 SSNs

Characteristics	n	%
Nodule size (mm)*	12.01±7.23	4–48
Size grouping		
<6 mm	4	4.82%
6≤ size <10 mm	38	45.78%
≥10 mm	41	49.40%
SSN type		
pGGN	48	57.83%
PSN	35	42.17%
Lesion location		
LUL	25	30.12%
RUL	22	26.51%
LLL	14	16.87%
RLL	18	21.96%
RML	4	4.82%
Air bronchogram	60	72.29%
Ill-defined margin	30	36.14%
Lobulation	23	27.71%
Pleural tail	33	39.76%
Spiculation	30	36.14%
Histologic type		
Benign	16	19.28%
AIS	23	27.71%
MIA	16	19.28%
IA	28	33.73%

*, data presented as mean ± standard deviation, range. SSN, subsolid nodule; SD, standard deviation; pGGN, pure ground-glass nodule; PSN, part-solid nodule; LUL, left upper lobe; RUL, right upper lobe; LLL, left lower lobe; RLL, right lower lobe; RML, right middle lobe; AIS, adenocarcinoma in situ; MIA, minimally invasive adenocarcinoma; IA, invasive adenocarcinoma.

infection in one patient, sclerosing pneumocytoma in one patient, and ciliated muconodular papillary tumor in one patient. Among the 67 lesions diagnosed as malignant, 23 were AIS, 16 were MIA, and 28 were IA.

Nodule malignancy

Table 3 compares the patient and nodule characteristics between benign and malignant samples. Malignant lesions were found to be more frequent in females (P=0.039), and have a significantly larger mean diameter (13.04±7.63 mm, median 10 mm) than benign lesions (7.7±2.18 mm, median 7.25 mm, P=0.0072) with an optimal cut-off of 9.24 mm [area under curve (AUC) =0.772; 95% confidence interval (CI): 0.654–0.891, sensitivity =0.612; specificity =0.812; *Figure 3*]. Characteristics found significantly more frequently in malignant lesions include air bronchograms (82.09% *vs.* 31.25%, P=0.000045), lobulation (32.84% *vs.* 6.25%, P=0.032781), pleural tail sign (46.27% *vs.* 12.5%, P=0.013147), and spiculation (43.28% *vs.* 6.25%, P=0.0056). These factors besides air bronchograms were further analyzed with multivariate logistic regression (AUC=87.36%) and showed that lesion size and speculation were independent risk factor for malignancy. Air bronchograms were excluded from further analysis due to multi-collinearity (*Table 4*).

Invasive adenocarcinoma

Due to its higher grade of malignancy and less favorable clinical prognosis, we compared the features of IA with those of its preinvasive and minimally invasive precursors (*Table 5*). A significant difference in the frequency of PSNs was noted between IA and AIS/MIA combined (67.86% *vs.* 23.08%, P=0.000247). In addition, IA was found to be significantly larger than AIS/MIA (16.16±9.16 *vs.* 10.79±5.42 mm, P=0.0038) with an optimal cut-off of 12 mm (AUC =0.724, 95% CI: 0.600–0.848, sensitivity =0.643; specificity =0.744, *Figure 4*). Other features found significantly more frequently in the IA group included pleural tail sign (75% *vs.* 25.64%, P=0.000064), air bronchograms (96.43% *vs.* 71.79%, P=0.009497), and lobulation (46.43% *vs.* 23.08%, P=0.0447). Spiculation showed borderline significance (57.14% *vs.* 33.33%, P=0.52376). Multivariate logistic regression (AUC =85.07%) showed that PSN presentation was a significant predictor for IA histology after controlling for smoking status, air bronchogram, pleural tail sign, spiculation, and lobulation (*Table 6*).

Discussion

With lung nodule cases, clinicians are confronted with the difficult task of differentiating between benign and malignant lesions based on imaging data. SSNs, in particular, pose a challenge as their indolence hinder

Table 3 Patient and nodule characteristics relative to nodule malignancy

Characteristics	Benign group (n=16)	Malignant group (n=67)	P value
Age (year)*	53.94±7.65	56.19±11.45	0.457
Sex			0.039
Male	10 (62.50%)	23 (34.33%)	
Female	6 (37.50%)	44 (65.67%)	
Smoking history			0.087
Never-smoker	11 (68.75%)	58 (86.57%)	
Ever-smoker	5 (31.25%)	9 (13.43%)	
Lesion multiplicity	2 (12.50%)	11 (16.42%)	0.698
History of malignancy	1 (6.25%)	14 (20.90%)	0.171
Nodule size (mm)*	7.7±2.18	13.04±7.63	0.007
Size grouping			0.002
<6 mm	3 (18.75%)	1 (1.49%)	
6≤ size <10 mm	10 (62.5%)	28 (41.79%)	
≥10 mm	3 (18.75%)	38 (56.71%)	
SSN type			0.887
pGGN	9 (56.25%)	39 (58.21%)	
PSN	7 (43.75%)	28 (41.79%)	
Lesion in upper lobe	9 (56.25%)	38 (56.72%)	0.973
Lesion location			0.692
LUL	5 (31.25%)	20 (29.85%)	
RUL	4 (25%)	18 (26.87%)	
LLL	4 (25%)	10 (14.93%)	
RLL	3 (18.75%)	15 (22.39%)	
RML	0	4 (5.97%)	
Air bronchogram	5 (31.25%)	55 (82.09%)	<0.001
Ill-defined margin	4 (25%)	26 (38.81%)	0.302
Lobulation	1 (6.25%)	22 (32.84%)	0.033
Pleural tail	2 (12.50%)	31 (46.27%)	0.013
Spiculation	1 (6.25%)	29 (43.28%)	0.006

*, data presented as mean ± standard deviation. n, number of cases; SSN, subsolid nodule; pGGN, pure ground-glass nodule; PSN, part-solid nodule; LUL, left upper lobe; RUL, right upper lobe; LLL, left lower lobe; RLL, right lower lobe; RML, right middle lobe; AIS, adenocarcinoma in situ; MIA, minimally invasive adenocarcinoma; IA, invasive adenocarcinoma.

prompt decision making. In this study, we analyzed the clinical and radiologic characteristics of Taiwanese patients and validated a number of malignancy features that could be applied to our practices.

Initial nodule size has long been used as a parameter for risk stratification (1). Our study demonstrated a significant difference in mean diameter between benign and malignant lesions, with an optimal cutoff point of 9.24 mm. We also

found that larger lesion size was indicative of IA histology, with an optimal cutoff of 12 mm. Only one out of five lesions smaller than 6 mm was found to be an AIS and classified as malignant, while 38 of 41 lesions larger than 10 mm were deemed malignant. This is in accordance with the 2017 Fleischner guidelines (7), which recommends close surveillance for nodules larger than 6 mm, and with previous studies (6,8,10-15), which found a size greater than 10 mm (or >8 mm) as an independent risk factor. Regarding the question of whether small malignant lesions were missed while only including patients who underwent surgical resection, the NLST and NELSON studies provide a large body of data relating to small nodules, both solid and subsolid (16,17). Aberle *et al.* presented the results of the two incidence screenings in NLST and showed that for nodules 4–6 mm in diameter, the positive predictive values were merely 0.3% and 0.7%. From the NELSON study, Horeweg *et al.* concluded that there was no difference in lung cancer risk between patients with a nodule smaller than 5 mm and patients with no nodules. In addition, the Fleischner guidelines and 2011 IASLC lung adenocarcinoma classification guidelines recommend surveillance only for SSNs larger than 6 mm due to the strong association of benign AAH with smaller nodules (4,7). Therefore, we are confident in the validity our findings, which should be minimally affected by external biases. As for nodules larger than 5 mm, Hiramatsu *et al.* (13) calculated a maximal distinguishing time-to-growth curve for pGGNs with an initial cut-off size of 10 mm, while other studies (12,18), like ours, have calculated a cut-off diameter of 8 to 12 mm for SSN invasiveness using ROC curve analysis.

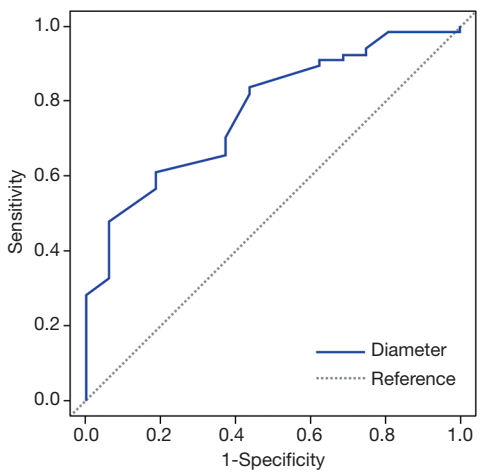

Figure 3 ROC curve of SSN malignancy related to lesion diameter. Area under curve (AUC) =0.772; optimal cut-off =9.24 mm; sensitivity =0.612; specificity =0.812. ROC, receiver operating characteristic; SSN, subsolid nodule.

In terms of radiologic characteristics, our results showed that air bronchograms (OR =10.08), lobulation (OR =7.33), pleural tail sign (OR =6.03), and spiculation (OR =11.45) were significant indicators of lesion malignancy, which concurs with prior literature. Air bronchograms (5,8,15,19) and bubble lucencies in SSNs have been associated with lepidic tumor growth along the bronchial wall. They are thought to be visualized through airway dilation, distortion secondary to retractile fibro-desmoplastic reaction, or alteration of wall elasticity (20). Lobulation (12,15,21,22) similarly is often attributed to the uneven cellular growth within neoplastic lung lesions. Spiculation, (2,7,8,12,23,24) and pleural tail signs (21,22) on the other hand, have been shown to represent malignant interstitium infiltrations accompanied with fibrosis and septal thickening.

Part-solid nodules (PSNs) play a pivotal role in current

Table 4 Multivariate logistic regression for nodule malignancy

Parameter	Estimate	Standard error	Odds ratio	95% CI	P value
Female sex	0.5832	0.3531	3.211	0.804–12.814	0.097
Nodule size	0.3801	0.1771	1.462	1.034–2.069	0.0318
PSN	–0.628	0.3871	0.285	0.062–1.299	0.1047
Pleural tail	0.3282	0.4982	1.928	0.273–13.59	0.5101
Spiculation	1.233	0.6157	11.775	1.054–131.57	0.0452
Lobulation	0.5571	0.6937	3.047	0.201–46.213	0.4219

AUC =87.36%; parameters included PSN, and those with P values less than 0.05 in *Table 3* except for air bronchogram. CI, confidence interval; PSN, part-solid nodule; AUC, area under curve.

Table 5 Comparison of characteristics between IA and AIS/MIA

Characteristics	AIS/MIA group (n=39)	IA group (n=28)	P value
Age (year)*	56.13±11.74	56.29±11.24	0.956
Nodule size (mm)*	10.79±5.42	16.16±9.16	0.004
Female sex	26 (66.67%)	18 (64.29%)	0.840
Ever-smoker	4 (10.26%)	5 (17.86%)	0.368
≥10 mm	17 (43.59%)	21 (75%)	0.010
PSN	9 (23.08%)	19 (67.86%)	<0.001
Air bronchogram	28 (71.79%)	27 (96.43%)	0.009
Ill-defined margin	14 (35.90%)	12 (42.86%)	0.564
Lobulation	9 (23.08%)	13 (46.43%)	0.045
Pleural tail	10 (25.64%)	21 (75%)	<0.001
Spiculation	13 (33.33%)	16 (57.14%)	0.052

*, data presented as mean ± standard deviation. n, number of cases; AIS, adenocarcinoma *in situ*; MIA, minimally invasive adenocarcinoma; IA, invasive adenocarcinoma; PSN, part-solid nodule.

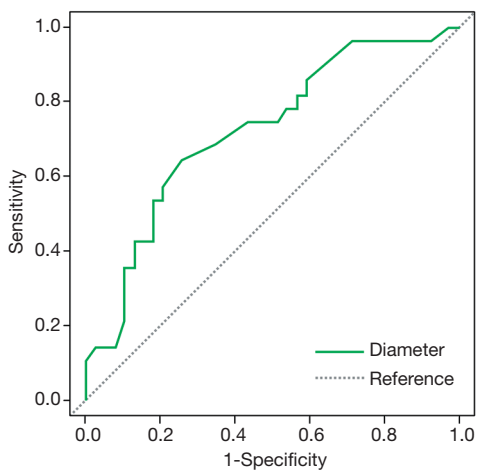

Figure 4 ROC curve of IA histology related to lesion diameter. Area under curve (AUC) =0.724; optimal cut-off for diameter =12 mm; sensitivity =0.643; specificity =0.744. ROC, receiver operating characteristic; IA, invasive adenocarcinoma.

guidelines, and have been extensively reported to be associated with malignancy, their size often correlating with the stage of disease progression (7). Our study did not indicate significant differences between benign and malignant PSNs possibly because we only selected lesions that were resected and already suspected of malignancy. However, we did find significantly higher rates of IAs presenting as PSNs (OR =7.04) when compared with AIS and MIA combined. This phenomenon has also appeared in previous studies (2,5,18,25). With regard to histological correlation, solid components in malignant SSNs have been shown to represent collapsed or mucin filled alveoli, fibroblastic proliferation, and stromal invasion (26).

Another feature we examined was ill-defined borders. Though not significant, an ill-defined border positively correlated with lesion malignancy (OR =1.90) and IA histology (OR =1.34). Previous literature regarding this attribute has shown varying and sometimes conflicting results. In general, benign pulmonary nodules tend to contain well-defined margins, whereas malignant nodules are more likely to exhibit vague edges. However, in the case of SSNs, well-defined borders have been reported to be associated with malignancy. Lee *et al.* (27) reported that PSNs found upon screening with ill-defined borders were more likely transient. Yang *et al.* (24) retrospectively reviewed 94 benign and 920 malignant resected SSNs and found that nodules with a well-defined border had a greater chance of malignancy. Multiple factors could have contributed to these discrepancies. For instance, whether a margin is considered well-defined or ill-defined is highly subjective and dependent on the observer. Another factor could be attributed to our specific selection criteria. In our study, the nodules have already undergone surveillance and we analyzed the set of images acquired immediately prior to surgical resection. Thus, our nodules with ill-defined borders can, in fact, be classified as a subgroup of

Table 6 Multivariate logistic regression for IA histology

Parameter	Estimate	Standard error	Odds ratio	95% CI	P value
Age	–0.0271	0.0325	0.973	0.913–1.037	0.405
Nodule size	0.0445	0.0493	1.046	0.949–1.151	0.366
Smoking	0.2451	0.5921	1.633	0.16–16.628	0.6789
PSN	0.7722	0.3229	4.685	1.321–16.611	0.017
Air bronchogram	–0.8079	0.6147	5.032	0.452–55.992	0.189
Pleural tail	–0.7632	0.4709	4.602	0.727–29.144	0.105
Spiculation	0.2482	0.3566	1.643	0.406–6.648	0.486
Lobulation	–0.2098	0.4165	0.657	0.128–3.363	0.614

AUC =85.07%; parameters included are age, smoking, and those with P values less than 0.2 in *Table 5*. IA, invasive adenocarcinoma; CI, confidence interval; PSN, part-solid nodule; AUC, area under curve.

persistent nodules, as opposed to transient ones. Lastly, we can entertain the possibility that the prevalence of specific imaging features varies among different populations, but more data is needed to generalize these findings.

Our study demonstrated a higher prevalence (60.24%), and also noted a significantly higher risk of malignancy in female patients (OR =3.19). This corresponds with other studies that have found predominance of persistent SSNs in females (14,27). Kobayashi *et al.* (28) reviewed nine reports with more than 100 SSNs and showed that among 1,973 patients with SSNs, 56% were female. They found this to be one of the shared features between SSNs and EGFR mutations among other factors such as non-smoker status and adenocarcinoma histology.

Lastly, one interesting finding regarding characteristic trends among different populations was that the average or median age of Asian patients with SSNs tends to be younger than their Western counterparts. The average age of our patient sample was 56 years. What's more, our three youngest patients, non-smoking females aged 28, 33 and 36 respectively, all had malignant lesions; the first two being IA and the third MIA. This is in accordance with the numerous reports that highlight the average age of Asian patients with SSNs ranging from the mid-fifties to the low-sixties (5,10-12,18,19,23,24). On the flipside, the general age range of studies that primarily focused on Caucasian populations fell between the high-sixties and seventies (29-33). Cohen *et al.* specifically studied Caucasian patients with PSNs and found a median age of 65 years old (25). Heidinger *et al.* studied 58 patients with adenocarcinoma spectrum lesions manifesting as pGGNs, among which 79% identified as "white". They found an average age of 68 years, and that 85% of white patients were current or ever-smokers, while only 1 out of 6 Asian patients was an ever-smoker (34). Various expert groups recommend LDCT screening for high risk individuals aged 55 to 74 with 30 pack-year history of smoking. Our findings, however, suggest that, among East Asian patients, even young individuals with no known risk factor, especially females, may benefit from LDCT screening. While this difference in patient age could be attributed to different selection criteria and screening accessibility, it may also be linked to specific features of lung cancer in never-smokers (LCNS). Nevertheless, it is increasingly evident that more tailored guidelines for different patient groups are necessary.

Our current study has several limitations. Since we specifically selected patients who underwent resection due to suspicion of malignancy, our patients' lesions may be larger and show more malignant traits. Furthermore, most patients were screened by self-referral and expenses were covered by the patients themselves, suggesting selection bias, but to an unknown extent. This was also a single-center retrospective study with a relatively small sample size; thus perhaps resulting in the variation of significant factors in univariate and multivariate analysis. Lastly, qualitative evaluation of imaging features remains highly subjective and prone to inter-observer variation. This calls for further research on computer-aided diagnosis (CAD) methods, which can facilitate nodule classification with more standardized measurements. Our results, however, concur with previous reports despite the aforementioned limitations. We were able to derive statistically significant findings while also validating previously reported indicators,

providing complementary data to the study of SSNs.

In conclusion, relatively young females with no known risk factor may be at risk of malignant SSNs in an East Asian population. CT features useful in identifying malignant SSNs included persistent nodules with diameters greater than or equal to 10 mm, part-solid components, air bronchograms, lobulation, pleural tail sign, and spiculation. Evaluating both imaging findings and patient factors such as sex and ethnicity can help clinicians make more accurate diagnoses and individualized management plans.

Acknowledgments

Funding: This work was financially supported by the "TMU Research Center of Cancer Translational Medicine" from The Featured Areas Research Center Program within the framework of the Higher Education Sprout Project by the Ministry of Education (MOE) in Taiwan. This work was supported by Health and welfare surcharge of tobacco products grant MOHW107-TDU-B-212-114020, MOHW107-TDU-B-212-114014 and MOHW107-TDU-B-212-114026B. This work was supported by Ministry of Science and Technology grant MOST 106-3114-B-038-001, MOST 107-2321-B-038-002, MOST 108-2321-B-038-003.

Footnote

Reporting Checklist: The authors have completed the STROBE reporting checklist. Available at http://dx.doi.org/10.21037/jtd-20-659

Data Sharing Statement: Available at http://dx.doi.org/10.21037/jtd-20-659

Peer Review File: Available at http://dx.doi.org/10.21037/jtd-20-659

Conflicts of Interest: All authors have completed the ICMJE uniform disclosure form (available at http://dx.doi.org/10.21037/jtd-20-659). All authors report grants from TMU Research Center of Cancer Translational Medicine, grants from Taiwan Ministry of Health and Welfare (MOHW), grants from Taiwan Ministry of Science and Technology grant (MOST), during the conduct of the study.

Ethical Statement: The authors are accountable for all aspects of the work in ensuring that questions related to the accuracy or integrity of any part of the work are appropriately investigated and resolved. This study was conducted in accordance with the Declaration of Helsinki (as revised in 2013) and approved by the Joint Institutional Review Board at Taipei Medical University (TMU-JIRB; No. N201909060). The requirement of informed consent was waived. The authors are accountable for all aspects of the work, including full data access, integrity of the data and the accuracy of the data analysis.

References

1. Naidich DP, Bankier AA, MacMahon H, et al. Recommendations for the management of subsolid pulmonary nodules detected at CT: a statement from the Fleischner Society. Radiology 2013;266:304-17.
2. McWilliams A, Tammemagi MC, Mayo JR, et al. Probability of cancer in pulmonary nodules detected on first screening CT. N Engl J Med 2013;369:910-9.
3. Yankelevitz DF, Yip R, Smith JP, et al. CT screening for lung cancer: nonsolid nodules in baseline and annual repeat rounds. Radiology 2015;277:555-64.
4. Travis WD, Brambilla E, Noguchi M, et al. International association for the study of lung cancer/American thoracic society/European respiratory society international multidisciplinary classification of lung adenocarcinoma. J Thorac Oncol 2011;6:244-85.
5. Lee SW, Leem CS, Kim TJ, et al. The long-term course of ground-glass opacities detected on thin-section computed tomography. Respir Med 2013;107:904-10.
6. Kobayashi Y, Sakao Y, Deshpande GA, et al. The association between baseline clinical–radiological characteristics and growth of pulmonary nodules with ground-glass opacity. Lung Cancer 2014;83:61-6.
7. MacMahon H, Naidich DP, Goo JM, et al. Guidelines for management of incidental pulmonary nodules detected on CT images: from the Fleischner Society 2017. Radiology

2017;284:228-43.
8. Cho J, Kim ES, Kim SJ, et al. Long-term follow-up of small pulmonary ground-glass nodules stable for 3 years: implications of the proper follow-up period and risk factors for subsequent growth. J Thorac Oncol 2016;11:1453-9.
9. Zhou W, Christiani DC. East meets West: ethnic differences in epidemiology and clinical behaviors of lung cancer between East Asians and Caucasians. Chin J Cancer 2011;30:287.
10. Kakinuma R, Noguchi M, Ashizawa K, et al. Natural history of pulmonary subsolid nodules: a prospective multicenter study. J Thorac Oncol 2016;11:1012-28.
11. Cho J, Ko SJ, Kim SJ, et al. Surgical resection of nodular ground-glass opacities without percutaneous needle aspiration or biopsy. BMC Cancer 2014;14:838.
12. Lee SM, Park CM, Goo JM, et al. Invasive pulmonary adenocarcinomas versus preinvasive lesions appearing as ground-glass nodules: differentiation by using CT features. Radiology 2013;268:265-73.
13. Hiramatsu M, Inagaki T, Inagaki T, et al. Pulmonary ground-glass opacity (GGO) lesions–large size and a history of lung cancer are risk factors for growth. J Thorac Oncol 2008;3:1245-50.
14. Silva M, Bankier AA, Centra F, et al. Longitudinal evolution of incidentally detected solitary pure ground-glass nodules on CT: relation to clinical metrics. Diagn Interv Radiol 2015;21:385.
15. Takahashi S, Tanaka N, Okimoto T, et al. Long term follow-up for small pure ground-glass nodules: implications of determining an optimum follow-up period and high-resolution CT findings to predict the growth of nodules. Jpn J Radiol 2012;30:206-17.
16. Aberle DR, DeMello S, Berg CD, et al. Results of the two incidence screenings in the National Lung Screening Trial. N Engl J Med 2013;369:920-31.
17. Horeweg N, van Rosmalen J, Heuvelmans MA, et al. Lung cancer probability in patients with CT-detected pulmonary nodules: a prespecified analysis of data from the NELSON trial of low-dose CT screening. Lancet Oncol 2014;15:1332-41.
18. Wu FZ, Chen PA, Wu CC, et al. Semiquantative visual assessment of sub-solid pulmonary nodules≦ 3 cm in differentiation of lung adenocarcinoma spectrum. Sci Rep 2017;7:15790.
19. Li M, Wang Y, Chen Y, et al. Identification of preoperative prediction factors of tumor subtypes for patients with solitary ground-glass opacity pulmonary nodules. J Cardiothorac Surg 2018;13:9.
20. Gaeta M, Caruso R, Blandino A, et al. Radiolucencies and cavitation in bronchioloalveolar carcinoma: CT-pathologic correlation. Eur Radiol 1999;9:55-9.
21. Fan L, Liu S, Li Q, et al. Multidetector CT features of pulmonary focal ground-glass opacity: differences between benign and malignant. Br J Radiol 2012;85:897-904.
22. Liang J, Xu X, Xu H, et al. Using the CT features to differentiate invasive pulmonary adenocarcinoma from pre-invasive lesion appearing as pure or mixed ground-glass nodules. Br J Radiol 2015;88:20140811.
23. Oh JY, Kwon SY, Yoon HI, et al. Clinical significance of a solitary ground-glass opacity (GGO) lesion of the lung detected by chest CT. Lung Cancer 2007;55:67-73.
24. Yang W, Sun Y, Fang W, et al. High-resolution Computed Tomography Features Distinguishing Benign and Malignant Lesions Manifesting as Persistent Solitary Subsolid Nodules. Clin Lung Cancer 2018;19:e75-83.
25. Cohen JG, Reymond E, Lederlin M, et al. Differentiating pre-and minimally invasive from invasive adenocarcinoma using CT-features in persistent pulmonary part-solid nodules in Caucasian patients. Eur J Radiol 2015;84:738-44.
26. Takashima S, Maruyama Y, Hasegawa M, et al. CT findings and progression of small peripheral lung neoplasms having a replacement growth pattern. AJR Am J Roentgenol 2003;180:817-26.
27. Lee SM, Park CM, Goo JM, et al. Transient part-solid nodules detected at screening thin-section CT for lung cancer: comparison with persistent part-solid nodules. Radiology 2010;255:242-51.
28. Kobayashi Y, Ambrogio C, Mitsudomi T. Ground-glass nodules of the lung in never-smokers and smokers: clinical and genetic insights. Transl Lung Cancer Res 2018;7:487-97.
29. Munir S, Koppikar S, Hopman WM, et al. Diagnostic Yield for Cancer and Diagnostic Accuracy of Computed Tomography–guided Core Needle Biopsy of Subsolid Pulmonary Lesions. J Thorac Imaging 2017;32:50-6.
30. Aherne EA, Plodkowski AJ, Montecalvo J, et al. What CT characteristics of lepidic predominant pattern lung adenocarcinomas correlate with invasiveness on pathology? Lung Cancer 2018;118:83-9.
31. Nelson DB, Godoy MC, Benveniste MF, et al. Clinicoradiographic predictors of aggressive biology in lung cancer with ground glass components. Ann Thorac Surg 2018;106:235-41.
32. Shewale JB, Nelson DB, Rice DC, et al. Natural history of ground-glass lesions among patients with previous lung

cancer. Ann Thorac Surg 2018;105:1671-7.
33. Digumarthy SR, Padole AM, Rastogi S, et al. Predicting malignant potential of subsolid nodules: can radiomics preempt longitudinal follow up CT? Cancer Imaging 2019;19:36.
34. Heidinger BH, Anderson KR, Nemec U, et al. Lung adenocarcinoma manifesting as pure ground-glass nodules: Correlating CT size, volume, density, and roundness with histopathologic invasion and size. J Thorac Oncol 2017;12:1288-98.

Cite this article as: Wang YH, Chen CF, Lin YK, Chiang C, Tzao C, Yen Y. Predicting malignancy: subsolid nodules detected on LDCT in a surgical cohort of East Asian patients. J Thorac Dis 2020;12(8):4315-4326. doi: 10.21037/jtd-20-659